SAND2022-10835C

Development of an Efficient Version of the Fuel Matrix Degradation Model

Jacob A. Harvey,* Anna M. Taconi,* Paul E. Mariner*

*Sandia National Laboratories, PO Box 5800, Albuquerque, NM 87123-0754 USA, jharve@sandia.gov

[leave space for DOI, which will be inserted by ANS]

INTRODUCTION

Degradation of spent nuclear fuel (UO_2) in a breached waste package occurs via a complex balance between chemical and oxidative dissolution. The overall process depends on several factors including the burnup and age of the fuel, environmental temperature, and concentration of dissolved species. Moreover, the process can be altered by the precipitation of solid species at the fuel surface which retards diffusional processes and restricts access to active sites. Noble metal particles can exist which catalytically speed up reaction processes. Modeling this complex process and predicting nuclear fuel dissolution rates is a difficult reactive-transport problem. This often becomes intractable when attempting to simulate hundreds or thousands of breached waste packages. To address this challenge, novel machine-learned surrogate models are highly attractive and the topic of on-going research. Surrogate models are dependent upon the data on which they are trained and therefore having a conservative but accurate process model for fuel dissolution rates is critical.

The Fuel Matrix Degradation (FMD) Model is the current capability being employed by the Spent Fuel and Waste Science and Technology (SFWST) campaign of the U.S. Department of Energy (DOE). The FMD model exists as a suite of MATLAB functions and subroutines which predicts the UO_2 dissolution rate via a 1-dimensional (1D) reactive-transport model. The current capabilities include alpha radiolysis of water for H_2O_2 generation, oxidative and chemical dissolution of the fuel matrix, additional redox reactions, aqueous chemical reactions, precipitation and dissolution of solid uranium, diffusional processes, and Arrhenius temperature dependencies.

We will show that the current implementation relies on a sequential iteration scheme to solve for interfacial corrosion potentials given static concentrations and subsequently solving for updated concentrations. We hypothesize that this leads to observed discontinuities in the predicted dissolution rate including a stair stepping behavior and static dissolutions rates at long times. At a minimum, the algorithm increases the number of non-linear solver iterations needed at each time step and increases the time required to generate new training data for future surrogate models. In this manuscript we propose a new algorithm for solving for the concentrations and corrosion potentials simultaneously while outlining our on-going efforts to improve the performance and reliability of the results predicted by the FMD model.

The remainder of this manuscript is organized as follows; first we detail the conceptual FMD model and describe the included processes, then we detail our results including identification of the computational bottleneck in the FMD model and proposed new algorithm, and lastly, we outline our conclusions and describe the current and on-going efforts.

FUEL MATRIX DEGRADATION MODEL SYSTEM AND PROCESSES

The FMD model is originally adapted from the mixed-potential model by Shoesmith et al.[1] The entirety of the model is better described elsewhere[2] however we will briefly orient the reader here to provide a common understanding. Fundamentally the FMD model exists to predict UO_2 fuel dissolution rates in a breached waste package and thereby provide a source term for performance assessment models. The MATLAB implementation simulates a 1D reactive transport column although it should be noted that 2D models are the subject of active research.[3] The system is depicted in Figure 1 where the left boundary represents the fuel surface, the right boundary is the breached container surface, which sandwich an aqueous region containing water and dissolved species. The aqueous region is spatially discretized with smaller spacings used near the interfaces.

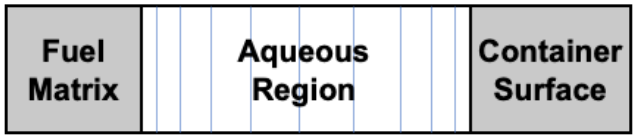

Figure 1. Physical model simulated by the FMD model which exists as a 1D reactive-transport column where the left boundary represents the fuel matrix, and the right boundary represents the breached container surface. A logarithmically discretized aqueous chemistry region is in the middle.

The aqueous chemistry reactions that are incorporated into the FMD model are shown in Table I while the electrochemical reactions that occur only at the fuel or container surface are shown in Table II. The fuel interface includes a noble metal particle region which has been shown to catalytically increase the reaction rate of the various reactions. Reaction rate expressions and associated

model parameters have been omitted here for clarity but can be found in previous reports.[4]

Table I. List of aqueous chemistry reactions incorporated in the FMD model.

Aqueous Chemistry Reactions
$UO_2^{2+} + 2OH^- + H_2O \rightarrow UO_3 \cdot 2H_2O$
$UO_2^{2+} + H_2O_2 + 4H_2O \rightarrow UO_4 \cdot 4H_2O + 2H^+$
$UO_2(CO_3)_2^{2-} + 2OH^- + H_2O \rightarrow UO_3 \cdot 2H_2O + 2CO_3^{2-}$
$UO_3 \cdot 2H_2O + 2CO_3^{2-} \rightarrow UO_2(CO_3)_2^{2-} + 2OH^- + H_2O$
$H_2O_2 + 2Fe^{2+} + 4OH^- \rightarrow 3H_2O + Fe_2O_3$
$O_2 + 4Fe^{2+} + 8OH^- \rightarrow 4H_2O + 2Fe_2O_3$
$UO_2^{2+} + 2Fe^{2+} + 6OH^- \rightarrow UO_{2,(aq)} + 3H_2O + Fe_2O_3$
$UO_2(CO_3)_2^{2-} + 2Fe^{2+} + 6OH^- \rightarrow UO_{2,(aq)} + 2CO_3^{2-} + 3H_2O + Fe_2O_3$
$H_2O_2 \rightarrow H_2O + \frac{1}{2}O_2$
$UO_{2,(s)} \rightarrow UO_{2,(aq)}$
$UO_{2,(aq)} \rightarrow UO_{2,(s)}$

Electrochemical reactions are implemented using the Mixed Potential Approach which works on two assumptions; (1) electrochemical reactions can be broken into partial oxidation/reduction reactions, and (2) there is no net accumulation of charge.[5] It is these electrochemical reactions that are the heart of the FMD model and lead to the oxidative dissolution of the fuel. As such they deserve outsized discussion here.

Each half reaction yields a current which depends on the fuel "corrosion potential". For example, the current for the first reaction in Table II ($UO_2 \rightarrow UO_2^{2+} + 2e^-$) is given by

$$i^{UO_2,1} = nF\varepsilon k_{UO_2,1} exp\left[\frac{\alpha_{UO_2,1}F}{RT}\left(E_{corr}^{UO_2} - E_{UO_2,1}^0\right)\right] \quad (1)$$

where n is the number of transferred electrons, F is Faraday's constant, ε is the porosity of fuel or steel corrosion layers, $k_{UO_2,1}$ is the reaction rate constant, $\alpha_{UO_2,1}$ is the electrochemical transfer coefficient, R is the universal gas constant, T is the temperature, $E_{corr}^{UO_2}$ is the corrosion potential of the fuel, and $E_{UO_2,1}^0$ is the standard potential. The central premise of the FMD model is that there is no net accumulation of charge or current, therefore

$$i_{anode} - i_{cathode} = 0. \quad (2)$$

Thus, at each timestep within a simulation, a set of ordinary differential equations are solved to determine $E_{corr}^{UO_2}$ at a given set of concentrations. This value of $E_{corr}^{UO_2}$ is then used to determine reaction rates and concentrations are updated using standard non-linear solvers (e.g., Newton-Rhapson).

Table II. Electrochemical reactions incorporated into the FMD model at the fuel, fuel noble metal particle (NMP), and steel (canister) interface.

Surface	Reactions
Fuel	$UO_2 \rightarrow UO_2^{2+} + 2e^-$
	$UO_2 + 2CO_3^{2-} \rightarrow UO_2CO_3^{2-} + 2e^-$
	$UO_2 \rightarrow UO_{2,(aq)}$
	$H_2 + 2OH^- \rightarrow 2H_2O + 2e^-$
	$H_2O_2 + 2OH^- \rightarrow O_2 + 2H_2O + 2e^-$
	$H_2O_2 + 2e^- \rightarrow 2OH^-$
	$O_2 + 2H_2O + 4e^- \rightarrow 4OH^-$
Fuel, NMP	$H_2 + 2OH^- \rightarrow 2H_2O + 2e^-$
	$H_2O_2 + 2e^- \rightarrow 2OH^-$
	$H_2O_2 + 2OH^- \rightarrow O_2 + 2H_2O + 2e^-$
	$O_2 + 2H_2O + 4e^- \rightarrow 4OH^-$
Steel	$Fe \rightarrow Fe^{2+} + 2e^-$
	$2H_2O + 2e^- \rightarrow H_2 + 2OH^-$

Hydrogen peroxide acts as the main oxidant within the FMD model (reaction 6, Table II) and is generated via radiolysis of groundwater. The treatment of radiolysis within the FMD model is relatively simple and the yield of H_2O_2 can be computed by

$$H_2O_2\ Yield = G_{H_2O_2} \times R_D(x,t) \times g(x) \quad (3)$$

where $G_{H_2O_2}$ is the generation value for H_2O_2, $R_D(x,t)$ is the dose rate, and $g(x)$ is a geometrical factor accounting for the fraction of fuel surface that is blocked from emitting

alpha radiation. In the current implementation, $G_{H_2O_2}$ is a constant value, however more complex expressions have been explored which depend on the concentration of H_2 and O_2. This is particularly relevant at low O_2 and high H_2 concentrations.[2] Radiolysis can also be enhanced by alpha emitters adsorbed in the porous solid uranium phases that form, however this effect is currently ignored.

The remaining notable process included in the FMD model is the precipitation of solid U phases at the fuel surface. This has a two-fold effect; (1) causing the retardation of diffusion near the fuel surface, and (2) blocking the availability of active sites for oxidative dissolution of the fuel.

Description of the Fortran Implementation of the FMD Model

We seek to refactor the FMD model code into a working version in Fortran. Our goal is to be more easily used and updated, as well as be readily modified for future corrosion applications. In this vein, we have begun developing, from scratch, a 1D reactive-transport code that implements the FMD model via a finite volume approach. We briefly describe that effort and the structure of the code here.

Diffusion is implemented by discretizing the system in space and time using a finite volume approach. Imagine a 3 grid cell system, with just 1 non-reactive diffusing species. The resulting governing equation is given by (ignoring advection, reaction, and source terms) $V\frac{(\phi C)_i^{k+1}-(\phi C)_i^k}{\Delta t} - \left(\phi AD\frac{C_i-C_{i-1}}{\Delta x}\right)_{i-\frac{1}{2}}^{k+1} + \left(\phi AD\frac{C_{i+1}-C_i}{\Delta x}\right)_{i+\frac{1}{2}}^{k+1} = 0 = f(C^{k+1,i})$, where k and k+1 are the current and new time step, V is the volume, ϕ is the porosity, C_i is the concentration in the ith grid cell, Δt is the time step, Δx is the distance between grid point centers, A is the area, and D is the diffusion coefficient. In this 1D case we will assume Δy and Δz are 1 and therefore V = Δx and A = 1. We will also assume a *full* grid cell exists at the boundaries. Concentrations are updated using the Newton-Raphson approach while a linear solver is used to solve the equation $J\delta C = -f(C^{k+1,i})$. Adding reactivity to the matrx form of this problem transforms the Jacobian matrix into a large (N_c * N_{grid}) × (N_c * N_{grid}) where N_c is the number of components and N_{grid} is the number of grid cells.

RESULTS

Here we will outline our results starting with the exploration of computational bottlenecks within the FMD model code, discussion of reaction rate parameters and their sensitivities, and lastly our current implementation of the alpha radiolysis.

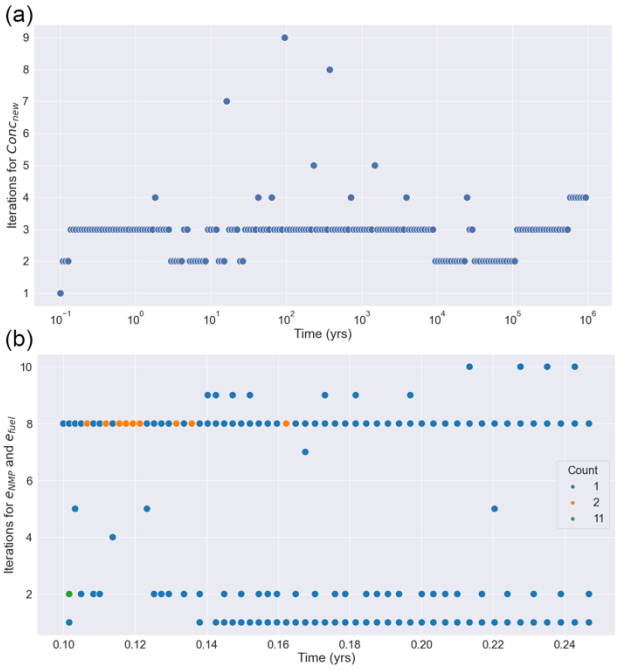

Figure 2. The number of Newton-Raphson iterations needed to solve for (a) the new concentrations and (b) the corrosion potentials at the fuel interface. The number of iterations needed for corrosion potentials are often the same and leads to overlapping points indicated by the colors in (b).

FMD Model Computational Bottleneck

As mentioned above, the corrosion potential provided in eq. 1 are solved given eq. 2 which generates a set of ordinary differential equations. Effectively this means the corrosion potentials are solved for given the current concentrations of various species within the system. The new corrosion potential is then used to update those concentrations and this process is iteratively continued until convergence is reached. Figure 2 depicts the number of Newton-Raphson iterations needed to solve for (a) new concentrations and (b) new corrosion potentials in a representative FMD model run using the MATLAB code. Recall that for each new set of concentrations, the corrosion potential needs to be updated. Therefore, for each time point there are several different sets of iterations to update the corrosion potential. For example, there are often 3 iterations needed to update new concentrations, for each of those 3 iterations there can be upwards of 8 iterations needed to solve for corrosion potentials, yielding 24 total iterations. Indeed, timing tests

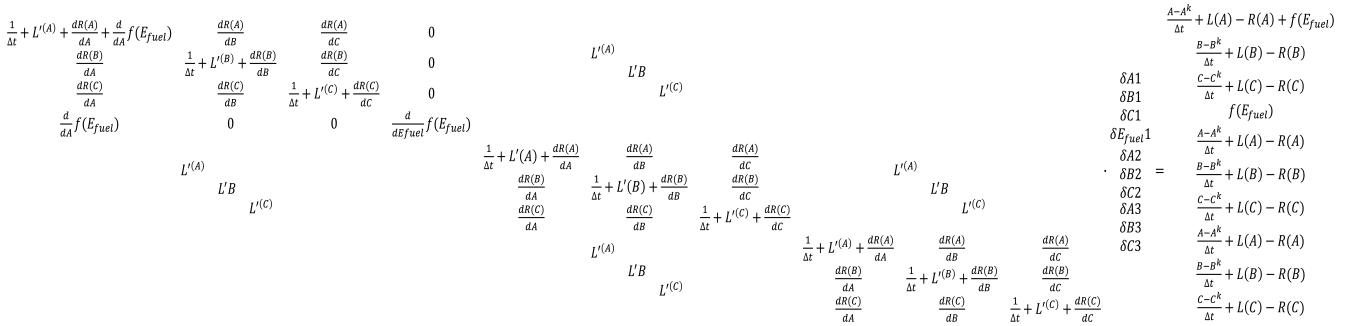

Figure 3. Representative proposed matrix for solving for corrosion potentials and new concentrations simultaneously in the FMD model. Here the reaction expressions and their derivatives are given by R, the diffusion operator is given by L, the corrosion potential equation is given by $f(E_{fuel})$, and the standard accumulation term for each species is $\frac{A-A^k}{\Delta t}$.

indicate that the FMD model code spends ~30% of the total computation time solving for corrosion potentials.

Herein we suggest a new algorithm that solves for corrosion potentials and new concentrations simultaneously. Imagine a 1D reactive transport system with 3 species (A + B → C) and 3 grid cells. Also assume that species A is accumulated via an electrochemical reaction with an associated corrosion potential (e.g., eq. 1). This electrochemical reaction only occurs in the left most grid cell (i.e., fuel surface). A typical matrix representation of the system solved via a finite volume method is shown in **Error! Reference source not found.**. In the 2nd and 3rd grid cell you observe the standard penta-diagonal structure in which the derivative of the rate expression for A, B, and C is taken with respect to the given species in the center 3 diagonals (e.g., $^{dR(A)}/_{dA}$), and the derivative of the diffusion operator (e.g., $L'(A)$) appears in the center and two off diagonals. The derivative of the standard accumulation term appears in the center diagonal (e.g., $^{1}/_{\Delta t}$). However, now given the need to solve for the corrosion potential and the concentration of A in the left most grid cell, the 3x3 block is transformed to a 4x4 block in the upper right. The 4th column represents the derivative of each reaction equation with respect to the corrosion potential. Note that this is 0 except for the 4th row in which the derivative of the corrosion potential equation is taken. The 4th row therefore has two entries, one in which the derivative of the fuel corrosion equation is taken with respect to the concentration of A and another where it is taken with respect to the corrosion potential itself. Using this matrix form, the corrosion potential and concentrations can be solved for simultaneously; potentially limiting unnecessary non-linear solver iterations, improving the efficiency of the algorithm, and removing observed discontinuities in the results.

Exploration of Model Parameter Sensitivities

Several of the reactions in Table 1 include a c_{sat} parameter in the rate expression. As we will lay out below, this parameter works to turn reactions off as the temperature decreases. For this case study, we will consider reaction 2 from Table 1 (i.e., $UO_2^{2+} + H_2O_2 + 4H_2O \rightarrow UO_4 \cdot 4H_2O + 2H^+$). This and only this reaction, will be turned on. A 5-grid cell system was considered with the initial concentrations of each species set to 0.01 M in the left most grid cell and 0 M in all other grid cells. In this system, the size of each grid cell is the same. The boundary condition at both the left and right boundaries was 0.01 M for all species. Diffusion was turned on, however $UO_4 \cdot 4H_2O$ is a solid and does not diffuse in the model.

The concentration of UO_2^{2+}as a function of time is shown as a log-log plot in Figure 4. Note that diffusion occurs at the left and right boundary and therefore, within a short period of time, the system is symmetric (i.e., grid cell 1 = grid cell 5). We note that the concentration of UO_2^{2+} reaches an initial equilibrium and the concentration remains relatively unchanged for ~100 years. At this point the concentration begins to increase towards that boundary condition concentration (i.e., 0.01 M) at ~1000 years.

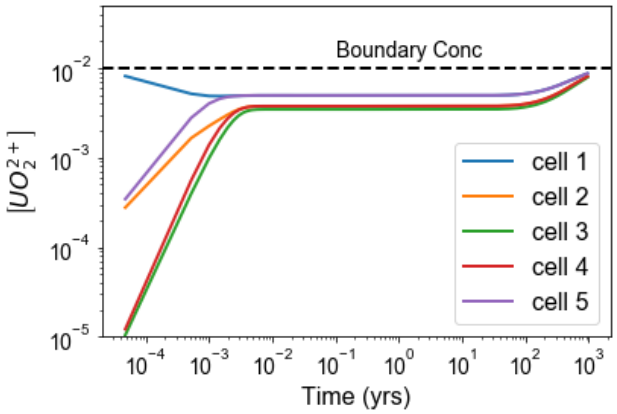

Figure 4. Concentration of UO_2^{2+} as a function of time in each of the 5 grid cells in our system.

In an effort to understand this nearly 100 year equilibrium we looked at the reaction rate constant for this reaction

$$k_2 = 1.0 \times 10^{-6} e^{6.0\times10^4 \cdot dT / \left(2.4 \cdot c_{sat}^{UO_2^{2+}}\right)^4} \quad (4)$$

and the $c_{sat}^{UO_2^{2+}}$ parameter

$$csat^{UO_2^{2+}} = 3.2 \times 10^{-2} \cdot e^{-3.0\times10^4 \cdot dT} \quad (5)$$

where $dT = \left(\frac{1}{298} - \frac{1}{T}\right)/R$ is an Arrhenius temperature factor. The reaction rate constant and $c_{sat}^{UO_2^{2+}}$ as a function of time are show in Figure 5. The temperature as a function of time is shown as an inset. Here we observe that the reaction rate constant is constant up until 100 years. At this point the temperature begins to decrease which leads to an increase in $c_{sat}^{UO_2^{2+}}$. Ultimately $c_{sat}^{UO_2^{2+}}$ increases by a factor of 2.3 from its initial value to its final value at the minimum temperature observed within this time period. However, the reaction rate constant has a $\left(c_{sat}^{UO_2^{2+}}\right)^4$ dependence meaning the rate constant decreases by a factor of 31. Therefore, the observed result that the concentration of UO_2^{2+} can go unchanged for 100 years can be explained by all the concentration that diffuses in from the boundary is immediately converted to $UO_4 \cdot 4H_2O$, however as the temperature decreases the reaction rate constant decreases rapidly. At this point, the rate of diffusion is greater than the rate of the reaction and the concentration of UO_2^{2+} begins to head toward the boundary condition. In this regard $c_{sat}^{UO_2^{2+}}$ works to, effectively, turn reactions off as the temperature of the system decreases at long times. Note that the temperature of the system is a simple analytical function however in the full FMD model UO_2^{2+} is produced due to corrosion at the fuel surface. Therefore, it is theoretical possible for the reaction rate to remain high despite a decreasing temperature if the concentration of UO_2^{2+} is large. This result indicates that long simulations are needed for the system to reach equilibrium. In an effort to meet this need we implemented an adaptive time stepping routine which scales the value of the time step based on the number of Newton-Raphson iterations needed to update the concentrations (i.e., a low number of iterations yields a longer time step).

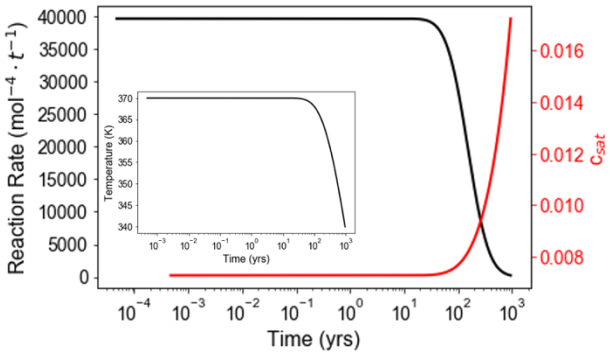

Figure 5. The reaction rate as a function of time for the reaction $UO_2^{2+} + H_2O_2 + 4H_2O \rightarrow UO_4 \cdot 4H_2O + 2H^+$ (right axis) and the $c_{sat}^{UO_2^{2+}}$ parameter (left axis). The inset shows the temperature as a function of time.

It is interesting to consider the reaction rate expressions and how they can affect the shape of the time evolution curves for various concentrations. Many of the reactions are 5th order with respect to a certain concentration. For example, reaction 3 and 4 from Table 1 are the reverse of each other, however reaction 3 has a rate constant that is, initially, 100X that of reaction 4. The rate expression for $UO_2(CO_3)_2^{2-}$ in reaction 3 is given by

$$\frac{\partial UO_2(CO_3)_2^{2-}}{\partial t} = -k_3[UO_2(CO_3)_2^{2-}]^5 \quad (6)$$

with

$$k_3 = 1.0 \times 10^{-4} e^{6.0\times10^4 \cdot dT / \left(2.4 \cdot c_{sat}^{UO_2(CO_3)_2^{2-}}\right)^4} \quad (7)$$

while for reaction 4 it is

$$\frac{\partial UO_2(CO_3)_2^{2-}}{\partial t} = k_4[CO_3^{2-}][UO_3 \cdot 2H_2O] \quad (8)$$

and

$$k_4 = 8.6 \times 10^{-6} e^{6.0\times10^4 \cdot dT} \quad (9)$$

This is due, in part, to the constant in front of the

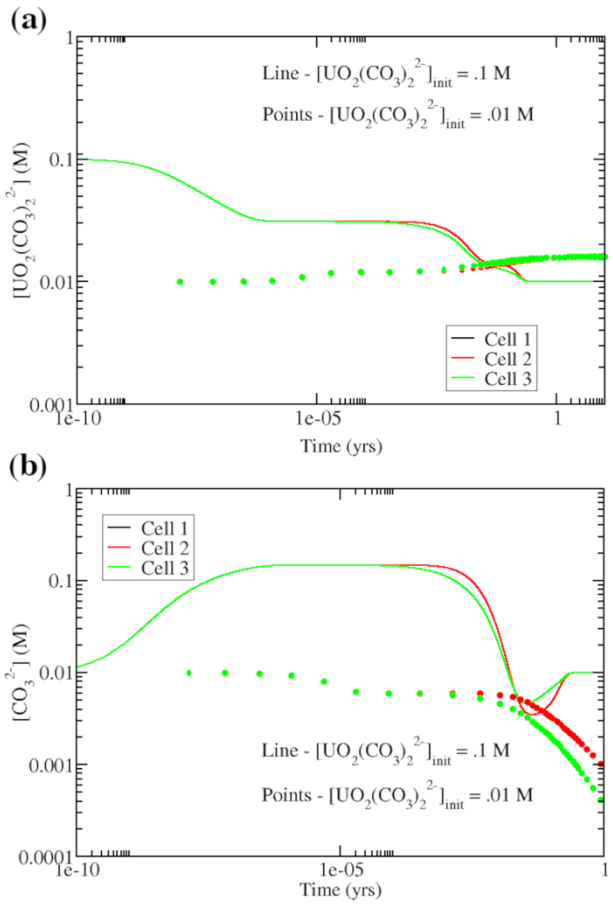

Figure 6. (a) $[UO_2(CO_3)_2^{2-}]$ and (b) $[CO_3^{2-}]$ as a function of time for a 3 grid cell simulation that tracks the first 4 reactions shown in Table 1. Two simulations are shown in which the initial $[UO_2(CO_3)_2^{2-}]$ concentration was .1 M (lines) and .01 M (points).

exponential but also due to the $c_{sat}^{UO_2(CO_3)_2^{2-}}$ parameter that appears in the rate constant for reaction 3 but not reaction 4. However, the rate expression has a 5th order dependence on $[UO_2(CO_3)_2^{2-}]$ (i.e., $\frac{\partial UO_2(CO_3)_2^{2-}}{\partial t} \propto [UO_2(CO_3)_2^{2-}]^5$).

We investigated this effect by considering a system containing 3 grid cells of equal length. The first 4 reactions from Table 1 were included. We ran two test cases, one in which the initial concentration of all species was .1 M and another where the initial concentration of all species was .01 M. The $[UO_2(CO_3)_2^{2-}]$ and $[CO_3^{2-}]$ as a function of time for both cases (lines = .1 M initial, points = .01 M initial) is shown in Figure 6. Note that the system is symmetric and therefore grid cells 1 and 3 are equal and therefore their curves are on top of each other. We note that different initial conditions can yield fundamentally different trajectories, and this is due, in large part, to the 5th order dependence. When the concentration of $UO_2(CO_3)_2^{2-}$ is low and raised to the 5th power the rate for reaction 3 where $UO_2(CO_3)_2^{2-}$ is consumed is small and therefore reaction 4 is faster and you see an increase in $[UO_2(CO_3)_2^{2-}]$ (points). Yet when the concentration is high, reaction 3 is faster and therefore you see a decrease in $[UO_2(CO_3)_2^{2-}]$ (line).

CONCLUSIONS

The computational bottleneck in the MATLAB-implemented FMD model has been identified using extensive timing studies. Significantly redundant Newton-Raphson iterations are being performed that can likely be reduced if the concentrations and corrosion potentials are solved for simultaneously. We have proposed a potential algorithm that could be used to achieve this and are currently working on implementation. We have shown, in great detail, how various reactions are controlled by certain parameters within the model and how initial and boundary conditions can significantly change the evolution of the system. Our current stand-along 1D reactive-transport code had included all bulk solution reactions, implements an adaptive time stepping routine, and is maintained via a gitlab repository with full version control. This effort is crucial for increasing the efficiency of surrogate model training on the FMD model

ACKNOWLEDGEMENTS

Sandia National Laboratories is a multi-mission laboratory managed and operated by National Technology and Engineering Solutions of Sandia, LLC., a wholly owned subsidiary of Honeywell International, Inc., for the U.S. Department of Energy's National Nuclear Security Administration under contract DE-NA-0003525.

This article has been authored by an employee of National Technology & Engineering Solutions of Sandia, LLC under Contract No. DE-NA0003525 with the U.S. Department of Energy (DOE). The employee owns all right, title and interest in and to the article and is solely responsible for its contents. The United States Government retains and the publisher, by accepting the article for publication, acknowledges that the United States Government retains a non-exclusive, paid-up, irrevocable, world-wide license to publish or reproduce the published form of this article or allow others to do so, for United States Government purposes. The DOE will provide public access to these results of federally sponsored research in accordance with the DOE Public Access Plan https://www.energy.gov/downloads/doe-public-access-plan.

This paper describes objective technical results and analysis. Any subjective views or opinions that might be expressed in the paper do not necessarily represent the views of the U.S. Department of Energy or the United States Government. SAND NO: SAND2022-8791 C

REFERENCES

1. D. W. Shoesmith, M. Kolar and F. King, Corrosion **59** (9), 802-816 (2003).
2. J. L. Jerden, K. Frey and W. Ebert, Journal of Nuclear Materials **462**, 135-146 (2015).
3. N. Liu, Z. Zhu, L. Wu, Z. Qin, J. J. Noël and D. W. Shoesmith, Corrosion **75** (3), 302-308 (2018).
4. J. L. Jerden, K. Frey, T. Cruse and W. Ebert, Report No. FCRD-UFD-2012-000169, 2012.
5. C. Wagner and W. Traud, Zeitschrift für Elektrochemie und angewandte physikalische Chemie **44** (7), 391-402 (1938).